

Predicting residual compressive strength of self-compacted concrete under various temperatures and relative humidity conditions by artificial neural networks

Ahmed M. Ashteyat^{*1} and Muhannad Ismeik^{1,2}

¹Department of Civil Engineering, The University of Jordan, Amman 11942, Jordan

²Department of Civil Engineering, Australian College of Kuwait, Safat 13015, Kuwait

(Received January 5, 2017, Revised June 24, 2017, Accepted October 2, 2017)

Abstract. Artificial neural network models can be successfully used to simulate the complex behavior of many problems in civil engineering. As compared to conventional computational methods, this popular modeling technique is powerful when the relationship between system parameters is intrinsically nonlinear, or cannot be explicitly identified, as in the case of concrete behavior. In this investigation, an artificial neural network model was developed to assess the residual compressive strength of self-compacted concrete at elevated temperatures (20-900°C) and various relative humidity conditions (28-99%). A total of 332 experimental datasets, collected from available literature, were used for model calibration and verification. Data used in model development incorporated concrete ingredients, filler and fiber types, and environmental conditions. Based on the feed-forward back propagation algorithm, systematic analyses were performed to improve the accuracy of prediction and determine the most appropriate network topology. Training, testing, and validation results indicated that residual compressive strength of self-compacted concrete, exposed to high temperatures and relative humidity levels, could be estimated precisely with the suggested model. As illustrated by statistical indices, the reliability between experimental and predicted results was excellent. With new ingredients and different environmental conditions, the proposed model is an efficient approach to estimate the residual compressive strength of self-compacted concrete as a substitute for sophisticated laboratory procedures.

Keywords: modeling; artificial neural network; residual compressive strength; self-compacted concrete; temperature; relative humidity

1. Introduction

Self-compacted concrete (SCC), also referred to as self-consolidating concrete, is one of the recent advances in concrete technology with increasing applications. This is a fresh concrete mix, developed in Japan in 1988, where the concrete is placed without internal or external vibration. The concrete is self-compacted with an ability to fill the formwork corners and tight areas between steel bars by gravity. For this to happen, SCC should be flowable with no segregation of coarse aggregates. Usage advantages of SCC include producing durable concrete, reduction in labor, expedited construction time, elimination of vibration processes and equipment, and production of better finished surfaces in areas of limited access and heavy reinforcements (Sonebi 2004).

Key components of SCC are similar to those ones used in conventional concrete. However, in order to maintain a sufficient flow, and cohesion and stability of the mix, an increase of the amount of powder materials as mineral additives, is usually utilized while manufacturing which reduces water-powder ratio. The increase in powder content is usually achieved by using pozzolana or less reactive filler

materials (Uysal 2012). Selection of most appropriate approach for producing SCC typically depends on the required strength and characteristics of the hardened concrete. With cement being the most expensive constituting component of concrete, reducing cement content may be considered as an economical alternative. Additionally, admixtures may improve particle packing and decrease the permeability of concrete which can improve its durability (Khayat *et al.* 2000, Khurana and Saccone 2001, Persson 2004). Moreover, certain industrial byproducts can be used as filler materials offering cost and environmental advantages. Typical examples include limestone, basalt, marble powder, fly ash, silica fume, quartz, granulated blast furnace slag, and glass (Yahia *et al.* 1999, Bouzoubaa and Lachemi 2001, Sonebi 2004, Ashteyat *et al.* 2012).

Concrete is recognized as an excellent thermal-resistant material among various construction materials, even though a major deterioration of concrete is noticed when it is exposed to a high temperature as in the case of fire (Xu *et al.* 2001, Ashteyat *et al.* 2014). Upon exposure to high temperatures, some of the physical and chemical properties may be affected in a nonreversible manner causing reduction in unit weight, modulus of elasticity, compressive strength, and formation of cracks and large pores on the surface (Janotka and Mojumdar 2005, Fares *et al.* 2009).

Concrete hydration, with an attendant release of heat, takes place at a temperature of up to 100°C. When

*Corresponding author, Ph.D.
E-mail: a.ashteyat@ju.edu.jo

temperature exceeds such a value, some dehydration may take place with an attendant absorption of heat. Dehydration reactions continue to a temperature in excess of 300°C. At a temperature range of 500 to 700°C, more significant reactions occur by dehydration of calcium hydroxide and decomposition of hydrate calcium silicate. At such temperatures, most changes experienced by concrete can be considered to be irreversible (Tanyildizi and Cevik 2010).

SCC features improve the internal structure of the material as compared to conventional concrete. However, the denser microstructure of SCC may be disadvantageous in a situation where SCC is exposed to fire. Experimental test results indicate that there is a huge difference between the properties of SCC and conventional concrete after being subjected to high temperatures as in the case of fire (Persson 2004, Annerel *et al.* 2007, Liu *et al.* 2008, Fares *et al.* 2009).

Residual compressive strength (RCS) is an important design parameter used to measure the durability of concrete when subjected to severe heat. Many investigations on the performance of SCC under high temperatures focused on RCS of concrete (Annerel *et al.* 2007, Fares *et al.* 2009, Haddad *et al.* 2013). Most of the research has shown that as the temperature reaches 300°C, a mild reduction in RCS is observed, however, as the temperature increases, a significant reduction in RCS is noticed. In addition, RCS is affected by relative humidity at intermediate temperatures between 300 and 400°C. However, as the temperature approaches 600°C, the effect of humidity becomes minimal. Relative humidity becomes more detrimental to strength at values greater than 80% (Haddad *et al.* 2013). The vapor destruction of pore internal system explains the higher damage of concrete at a higher relative humidity. The drastic reduction in the influence of relative humidity on RCS at a temperature greater than 500°C is due to the damage induced by the destruction of bindery material in the hydrated cement (Neville 1996).

Fibers are often used to overcome the adverse effect of fire induced spalling (Khaliq and Kodur 2011). Polypropylene fiber and steel fiber have been used in SCC exposed to fire in order to reduce the effect of spalling (Persson 2004, Fares *et al.* 2009, Tao *et al.* 2010, Ding *et al.* 2012). Polypropylene fibers shrink and melt when heated to a temperature above 170°C and create randomly oriented micro and macro channels inside concrete resulting in a slightly more porous concrete (Kalifa *et al.* 2001, Noumowe *et al.* 2006, Khaliq and Kodur 2011). These channels and

the higher porosity can contribute to the relief of high internal moisture pressures at elevated temperatures thus decreasing fire spalling. Addition of steel fibers may compensate for the brittle nature and may enhance the tensile strength and toughness of SCC before, during, and after exposure to high temperatures. Although fibers showed an improvement in reducing fire spalling, many of the experimental research on SCC showed a decrease in RCS of concrete at elevated temperatures (Liu *et al.* 2008).

Artificial neural network (ANN) technology, a sub-field of artificial intelligence, is often applied to solve various civil engineering problems. ANNs are a useful tool for information processing and many other applications. Unlike linear regression modeling in civil engineering (Ismeik 2010, Aktas and Ozerdem 2016), ANNs can be used to solve complex problems that cannot be handled by analytical approaches or with problems whose underlining physical and mathematical models are not well-known (Fausett 1994).

ANN models have been used in material modeling and behavior prediction (Chiang and Yang 2005, Alshihri *et al.* 2009, Bilim *et al.* 2009, Gregor *et al.* 2009, Atici 2011, Siddique *et al.* 2011, Ismeik and Al-Rawi 2014, Duan and Poon 2014, Engin *et al.* 2015, Soneibi *et al.* 2016, Camoes and Martins 2017). The available research in the literature modeled the conventional concrete strength under selected conditions with limited attention to a comprehensive modeling approach to RCS of SCC. Therefore, the lack of knowledge in this direction is obvious.

The aim of this study is to build a general model to predict RCS of SCC exposed to elevated temperatures and high relative humidity conditions. For purpose of constructing the model, training, testing, and validation using the available experimental results of 332 concrete mixes were gathered from the technical literature.

2. Methods and materials

2.1 Artificial neural networks

An ANN is as a massively parallel distributed processor, made up of simple processing units, that has a natural propensity for storing experiential knowledge and making it available for use. It resembles the brain in two aspects 1) knowledge is acquired by the network from this environment through a learning process, and 2) interneuron

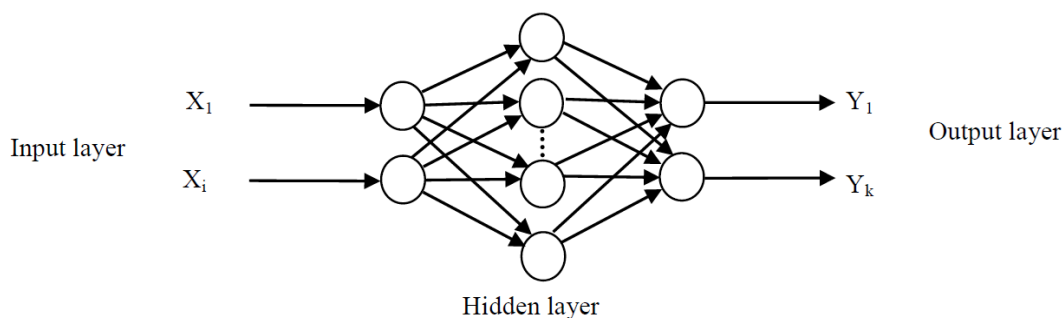


Fig. 1 A typical structure of an artificial neural network

connections strengths, known as synaptic weights, are used to store the acquired knowledge (Haykin 1999).

The interest in ANNs is due to their capability to simulate natural intelligence in its learning from past experience. The method generally relies on experimental results, which are used to train the ANN model so that it can precisely predict system performance at other conditions.

A typical ANN architecture is composed of at least three layers interconnected through some sort of processing elements known as neurons as shown in Fig. 1. The input layer contains input variables $x_1, x_2,$ and x_i , while the output layer contains output variables $y_1, y_2,$ and y_k . The hidden layer consists of a number j neurons connected to each input x_i and output y_k . A neuron consists of weight, bias, and a transfer function. Each neuron receives an input x_i attached with a weight w_{ij} and a bias b_i to obtain a weighted sum which then is passed through a nonlinear activation function as given by Eq. (1). The output y_k is then obtained as given in Eq. (2).

$$u_j = f\left(\sum_i (w_{ij}x_i + b_j)\right) \quad (1)$$

$$y_k = \sum_j (W_{jk}u_j) + B_k \quad (2)$$

In the above equations, w_{ij} is a weight linking the input variable x_i to hidden neuron value u_j , W_{jk} is a weight linking the hidden neuron value u_j to the output y_k , b_j is the value of the bias of hidden neuron j , B_k is the value of the bias of output y_k , and f is the activation function which transforms the weighted linear combination of inputs and the bias term into the value of neuron u_j . Usually, the transfer function serves to introduce the nonlinearity into the model. It may be of any form, and the one used in this study was the logarithmic function.

ANNs can be trained to reach from a particular input to a specific target output using the back-propagation algorithm. This is done through modifying the weights and biases of the network until the error between network output and experimental value is minimized. When the error falls below a specific range or maximum number of epochs are exceeded, the training process is usually terminated. The rate of this iterative procedure is controlled by a momentum term and a learning rate which are between 0 and 1. If convergence occurs, the trained network is able to estimate the results of other new original experiments (Rumelhart *et al.* 1986).

Determining a proper structure for a network is an important issue since network topology greatly affects its simulation capability. In this investigation, trial-and-error approach was used to obtain the best architecture of the network by evaluating different number of transfer functions and neurons. Training was terminated when 50000 epochs were reached or until the error over all training iterations was minimized to a stable value of less than 0.001.

Performance of an ANN-based prediction is evaluated by several statistical indices and by a regression analysis between the predicted outputs and corresponding

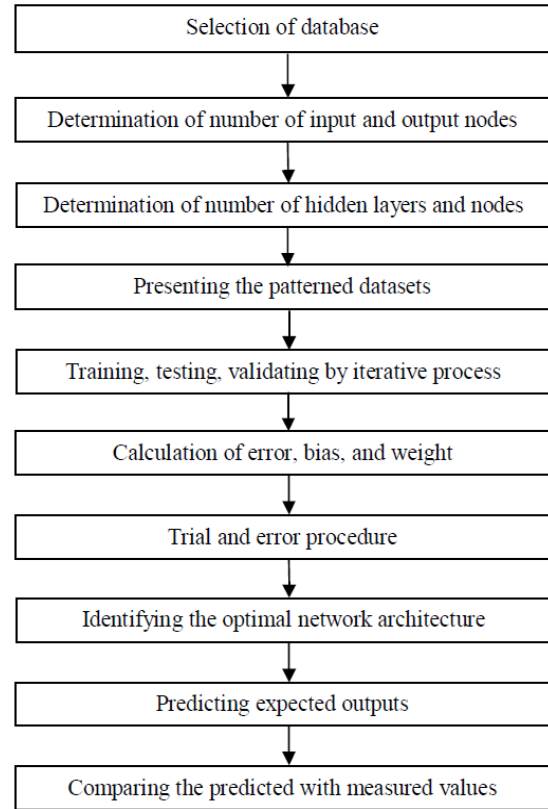


Fig. 2 ANN model development steps (Fausett 1994)

experimental values. In this study, a large number of different networks were tested and statistically monitored. The one with highest strength was selected as it represented the best generalization.

A typical flowchart of the major steps of developing an ANN model is presented in Fig. 2. For further details, a comprehensive description of ANN structures is given by Fausett (1994).

2.2 Experimental database

In order to build a comprehensive database, experimental results of 9 different sources, as reported in the literature, were used to develop the ANN model (Anagnostopoulos *et al.* 2009, Fares *et al.* 2009, Tao *et al.* 2010, Bakhtiyari *et al.* 2011, Khaliq and Kodur 2011, Ding *et al.* 2012, Uysal 2012, Uysal *et al.* 2012, Haddad *et al.* 2013).

RCS was the key output parameter in this study. The 18 input independent variables considered for model development were classified into 4 categories. First category was concrete ingredients such as cement (C), water (W), fine aggregate (FA), coarse aggregate (CA), water-to-cement ratio (WC), and super plasticizer dosage (SP). Second category was filler type such as silica fume (SF), slag (SG), fly ash (FAS), marble (M), basalt (B), limestone (LS), glass (G), and quartz (Q). Third category was fiber type such as polypropylene (PP), and steel fiber (ST). Fourth category was environmental conditions such as relative humidity (RH), and temperature (T). The collected experimental data consisted of 332 sets, in which 234 sets

Table 1 Sample of the data used for model development as obtained from literature

C	W	FA	CA	WC	SP	SF	SG	FAS	M	B	LS	G	Q	PP	ST	RH	T	RCS	Reference
467	182	865	762	0.39	9.85	0	0	83	0	0	0	0	0	0	0	95	20	100	
467	182	865	762	0.39	9.85	0	0	83	0	0	0	0	0	0	0	95	200	103.1	
467	182	865	762	0.39	9.85	0	0	83	0	0	0	0	0	0	0	95	400	84	
440	182	863	772	0.41	9.63	0	0	0	0	110	0	0	0	2	0	95	400	73	
440	182	863	772	0.41	9.63	0	0	0	0	110	0	0	0	2	0	95	600	43	Uysal (2012)
440	182	863	772	0.41	9.63	0	0	0	0	110	0	0	0	2	0	95	800	18	
440	182	865	774	0.37	9.08	0	0	0	110	0	0	0	0	0	0	95	20	100	
440	182	865	774	0.37	9.08	0	0	0	110	0	0	0	0	0	0	95	600	51	
440	182	865	774	0.37	9.08	0	0	0	110	0	0	0	0	0	0	95	800	20.8	
320	175	1021	626	0.55	4.32	0	0	0	0	0	0	0	185	0	0	42	20	100	
320	175	1021	626	0.55	4.32	0	0	0	0	0	0	0	185	0	0	42	150	103	Bakhtiyari et al. (2011)
320	175	1021	626	0.55	4.32	0	0	0	0	0	0	0	185	0	0	42	500	118.7	
372	160	1029	629	0.43	5.76	28	0	0	0	0	0	0	120	0	0	42	500	136	
372	160	1029	629	0.43	5.76	28	0	0	0	0	0	0	120	0	0	42	750	0	
340	188	825	800	0.55	6.13	0	135	0	0	0	0	0	0	0	0	65	20	100	
340	188	825	800	0.55	6.13	0	135	0	0	0	0	0	0	0	0	65	300	85.3	
375	189	862	800	0.5	8.27	0	100	0	0	0	0	0	0	0	0	65	300	81.6	Anagnostopoulos et al. (2009)
375	189	862	800	0.5	8.27	0	100	0	0	0	0	0	0	0	0	65	600	43.7	
380	194	862	800	0.51	5.62	0	0	0	0	0	0	100	0	0	0	65	300	80	
380	194	862	800	0.51	5.62	0	0	0	0	0	0	100	0	0	0	65	600	44.3	
400	160	547.32	710	0.4	11.6	0	0	0	0	0	75	0	0	0	0	28	20	100	
400	160	547.32	710	0.4	11.6	0	0	0	0	0	75	0	0	0	0	28	300	80.1	
400	160	547.32	710	0.4	11.6	0	0	0	0	0	75	0	0	0	0	28	400	55	
400	160	547.32	710	0.4	11.6	0	0	0	0	0	75	0	0	0	0	28	500	42.2	
400	160	547.32	710	0.4	11.6	0	0	0	0	0	75	0	0	0	0	28	600	16.1	Haddad et al. (2013)
400	160	547.32	710	0.4	11.6	0	0	0	0	0	75	0	0	0	0	58	20	100	
400	160	547.32	710	0.4	11.6	0	0	0	0	0	75	0	0	0	0	58	300	75.3	
400	160	547.32	710	0.4	11.6	0	0	0	0	0	75	0	0	0	0	58	400	46.7	
400	160	547.32	710	0.4	11.6	0	0	0	0	0	75	0	0	0	0	58	600	16	

Table 2 Descriptive statistics of database variables

Var.	Unit	Range	Min	Max	Mean	S. Dev.	Variation	Skewness
<i>Concrete ingredients</i>								
C	kg/m ³	330.00	220.00	550.00	398.10	70.62	0.18	0.06
W	kg/m ³	79.00	143.00	222.00	180.51	17.69	0.10	0.18
FA	kg/m ³	481.68	547.32	1029.00	801.40	123.51	0.15	-0.87
CA	kg/m ³	278.00	626.00	904.00	758.06	56.23	0.07	0.52
WC	-	0.50	0.33	0.83	0.47	0.10	0.21	1.62
SP	kg/m ³	11.66	1.64	13.30	7.92	2.32	0.29	-0.69
<i>Filler types</i>								
SF	kg/m ³	28.00	0.00	28.00	0.67	4.29	6.36	6.24
SG	kg/m ³	330.00	0.00	330.00	27.50	70.84	2.58	3.03
FAS	kg/m ³	193.00	0.00	193.00	27.00	51.33	1.90	1.68
M	kg/m ³	165.00	0.00	165.00	9.94	34.30	3.45	3.59
B	kg/m ³	165.00	0.00	165.00	11.45	35.99	3.14	3.22
LS	kg/m ³	225.00	0.00	225.00	47.68	65.94	1.38	1.01
G	kg/m ³	130.00	0.00	130.00	2.08	15.45	7.43	7.46
Q	kg/m ³	185.00	0.00	185.00	3.67	23.92	6.51	6.66
<i>Fiber types</i>								
PP	kg/m ³	3.00	0.00	3.00	0.63	0.91	1.44	0.89
ST	kg/m ³	55.00	0.00	55.00	3.81	12.68	3.33	3.13
<i>Environmental conditions</i>								
RH	%	71.00	28.00	99.00	84.92	18.14	0.21	-1.69
T	C	880.00	20.00	900.00	386.14	267.94	0.69	0.10
<i>Output variable</i>								
RCS	%	136.00	0.00	136.00	65.29	30.69	0.47	-0.32

(70%) were used for training, 49 sets (15%) were used for testing, and 49 sets (15%) were used for validation. Due to the large amount of data used, a selected sample is presented in Table 1 with a descriptive statistics of all variables shown in Table 2.

3. Results and discussion

The RCS of SCC subjected to elevated temperatures and different humidity levels was predicted using ANN modeling. A multi-layered feed-forward neural network, with back-propagation algorithm, was employed during the analysis. The number of neurons, in the hidden layer, was determined by training a large number of networks with different numbers of hidden neurons while comparing the predicted results with experimental values to obtain the optimal structure. A source code was used to develop a relatively large number of different ANN configurations. With a trial-and-error approach, the code optimized the number of neurons and selection of transfer functions.

Estimation of RCS was developed using the experimental database as obtained from literature. Input parameters were C, W, FA, CA, WC, SP, SF, SG, FAS, M, B, LS, G, Q, PP, ST, RH, and T, while the output variable was RCS. As seen in Fig. 3, the 18-5-1 structure (eighteen input neurons, five neurons in one hidden layer, one output

Table 3 ANN model structure and performance

Model properties				
Output	Input	Structure	Function	
RCS	C, W, FA, CA, WC, SP, SF, SG, FAS, M, B, LS, G, Q, PP, ST, RH, T	18-5-1	Log-Log	
Training parameters				
R^2	MAE	RMSE	MAPE	E
0.9686	3.5996	5.2939	7.2095	0.9229
Testing parameters				
R^2	MAE	RMSE	MAPE	E
0.9330	5.5611	7.9537	11.8489	0.8481
Validation parameters				
R^2	MAE	RMSE	MAPE	E
0.8566	7.0491	12.8482	13.1386	0.7264
All datasets parameters				
R^2	MAE	RMSE	MAPE	E
0.9443	4.3862	7.2553	48.8351	0.8775

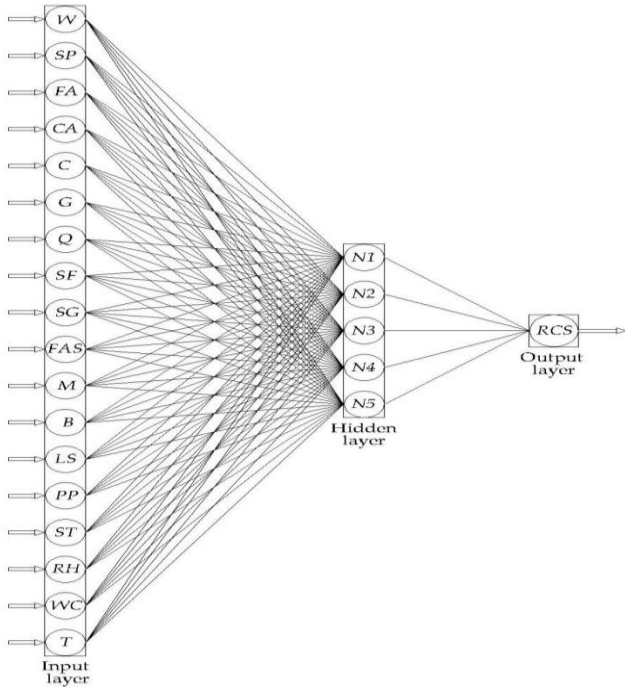


Fig. 3 Optimal ANN architecture

neuron) was found to be the optimal architecture. The momentum term and learning rate were taken as 0.3 and 0.1, respectively. Input and output transfer functions were logarithmic as shown in Table 3 while biases and connection weights were listed in Table 4.

The developed model was evaluated for statistical performance using the coefficient of determination (R^2), mean absolute error (MAE), root mean square error (RMSE), mean absolute percentage error (MAPE), and coefficient of efficiency (E) as defined by Eqs. (3) to (7). Strength of the model was measured for the training, testing, and validation data as well as for all datasets as reported in Table 3. In these equations, Z_k is the

Table 4 ANN model biases and connection weights (18-5-1)

	N_1	N_2	N_3	N_4	N_5	RCS
C	1.7881	0.7017	-0.1622	-0.3071	-2.0436	
W	0.3700	0.1645	-0.8582	0.6523	-0.4721	
FA	0.1687	-0.1510	0.2316	0.0110	-0.0854	
CA	-0.3361	0.1978	-4.5333	0.2091	0.4496	
WC	0.0054	0.3153	-0.6198	-0.6994	-0.5505	
SP	0.3959	-0.5134	0.1886	0.1772	-0.8565	
SF	-8.0550	0.1357	-0.5326	0.8750	0.6785	
SG	0.4635	-0.1897	-0.7968	-0.1007	-0.1526	
FAS	0.1319	0.1752	0.0871	-0.1941	-0.3966	
M	-0.0270	-0.1526	0.3349	-2.7270	1.1068	
B	-0.2764	1.4854	-0.5297	-0.0364	-0.0477	
LS	0.8769	0.9512	-0.0302	-0.3124	0.4501	
G	0.1991	-0.5678	-0.3384	0.4468	0.2055	
Q	0.1456	1.6166	0.5952	-1.9716	1.7865	
PP	0.4769	-0.3522	-1.5571	-0.5194	0.8609	
ST	0.1609	0.1916	0.0369	-0.8867	-1.8306	
RH	0.5531	-0.6221	0.0720	-0.3916	-0.9210	
T	-1.2643	-0.4972	1.7621	-2.1104	7.6217	
RCS	0.9552	-5.7158	6.0542	-2.3418	-5.2100	
Bias	0.1464	1.7709	1.2364	0.7788	-1.6368	2.9852

experimental RCS, Y_k is the predicted RCS, k is a counter, and N is the number of dataset.

$$R^2 = \frac{(\sum_{k=1}^N (Z_k - \bar{Z})(Y_k - \bar{Y}))^2}{\sum_{k=1}^N (Z_k - \bar{Z})^2 \sum_{k=1}^N (Y_k - \bar{Y})^2} \quad (3)$$

$$MAE = \frac{1}{N} \sum_{k=1}^N |Z_k - Y_k| \quad (4)$$

$$RMSE = \sqrt{\frac{1}{N} \sum_{k=1}^N (Z_k - Y_k)^2} \quad (5)$$

$$MAPE = \frac{1}{N} \left[\frac{\sum_{k=1}^N |Z_k - Y_k|}{\sum_{k=1}^N Z_k} \times 100 \right] \quad (6)$$

$$E = \frac{[\sum_{k=1}^N (Z_k - \bar{Z})^2 - \sum_{k=1}^N (Y_k - Z_k)^2]}{[\sum_{k=1}^N (Z_k - \bar{Z})^2]} \quad (7)$$

As listed in Table 3, a high prediction capability was obtained for the training, testing, and validation datasets as verified by the statistical indices. The R^2 , MAE, RMSE, MAPE, and E values for the training dataset were 0.9686, 3.5996, 5.2939, 7.2095, 0.9229; for the testing dataset were 0.9330, 5.5611, 7.9537, 11.8489, 0.8481; and for the validation dataset were 0.8566, 7.0491, 12.8482, 13.1386, 0.7264, respectively. Thus, the proposed ANN model offered excellent performance capability of predicting RCS of SCC accurately with the selected input variables.

To have a more precise investigation into the model, a comparison between experimental results and predicted values of RCS of SCC for the training, testing, and validation datasets was plotted. As illustrated by Figs. 4, 5, and 6, an excellent agreement existed between experimental and predicted values for the three datasets. This demonstrated that the suggested ANN model was successful in learning and capturing the relationship between the input parameters (C, W, FA, CA, WC, SP, SF, SG, FAS, M, B, LS, G, Q, PP, ST, RH, T) and the output variable (RCS).

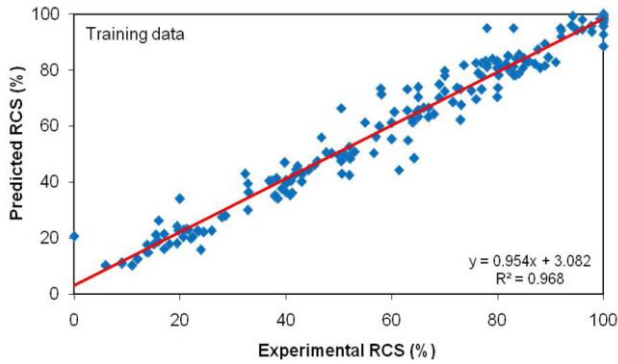


Fig. 4 Comparison between predicted and experimental values of RCS of training data

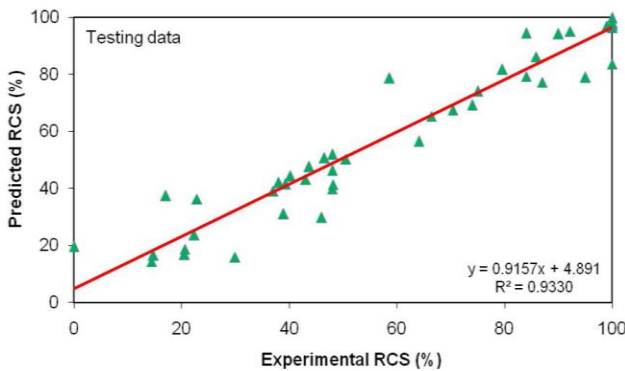


Fig. 5 Comparison between predicted and experimental values of RCS of testing data

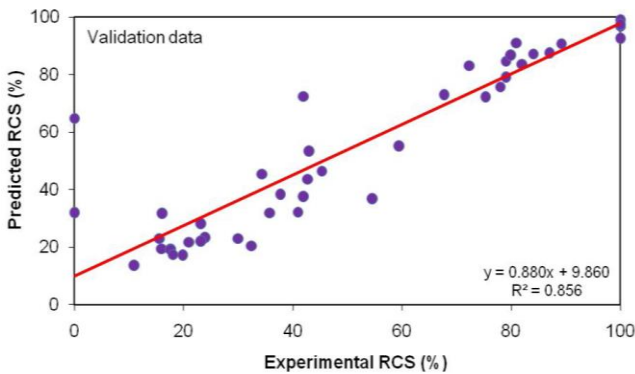


Fig. 6 Comparison between predicted and experimental values of RCS of validation data

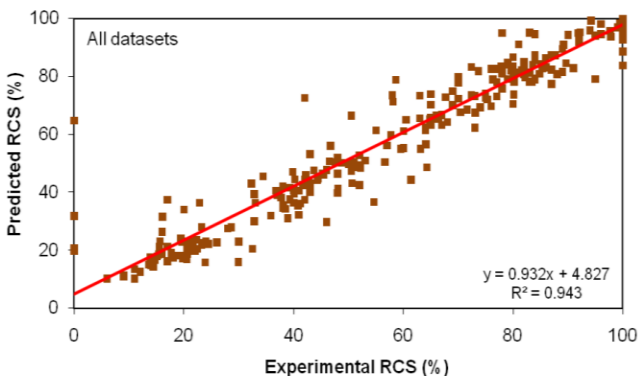


Fig. 7 Comparison between predicted and experimental values of RCS of all datasets

Table 5 Statistical comparison between experimental data and ANN model prediction

Parameter	Experimental RCS (%)	Predicted RCS (%)	Variation (%)
Range	136.0000	107.9956	20.5915
Min	0.0000	10.2780	NA
Max	136.0000	118.2737	13.0341
Mean	65.2946	65.7057	0.6296
Std. Deviation	30.6920	29.4593	4.0163
Coef. of Variation	0.4701	0.4484	4.6168
Skewness	-0.3178	-0.3111	2.0981
R^2	1.0000	0.9443	5.5681

4. Model assessment

A graphical illustration between predicted outputs and experimental values of RCS for all datasets is given in Fig. 7. Inclination of the best fit is almost 45° which means that the proposed model prediction capability is excellent; especially with the clear absence of outliers. The R^2 , MAE, RMSE, MAPE, and E values for all datasets were 0.9443, 4.3862, 7.2553, 48.8351, and 0.8775, as cited from Table 3.

A comparison in terms of statistical performance of the proposed model is believed to be useful. The statistical parameters range, min, max, mean, standard deviation, coefficient of variation, skewness, and coefficient of determination were used as a comparison tool. As seen in Table 5, the deviation between experimental and predicted values was relatively small. Thus, the ANN model outcome had a close distribution properties as compared to experimental values.

5. Conclusions

Self-compacted concrete is a nonlinear material, so modeling its performance under severe environmental conditions is a highly difficult task. An investigation was undertaken to develop an artificial neural network model that could be employed feasibly for estimating residual compressive strength of self-compacted concrete. Input parameters were concrete ingredients, filler type, fiber type, and environmental conditions. A multi-layered feed-forward neural network model was used. Model architecture consisted of eighteen input neurons, five neurons in one hidden layer, and one output neuron. The adopted model was developed based on a reliable experimental data obtained from the technical literature. Residual compressive strength values predicted using the proposed model were very close to experimental results as illustrated by statistical indices.

The present study shows that the determination of residual compressive strength of self-compacted concrete at elevated temperatures, and different humidity conditions, can be predicted accurately and reliably using the proposed artificial neural network model. Since concrete experimental testing requires specialized equipment and

expertise, the use of suggested model can be an alternative tool for estimating residual compressive strength of self-compacted concrete efficiently and reliably.

References

- Aktas, G. and Ozerdem, M.S. (2016), "Prediction of behavior of fresh concrete exposed to vibration using artificial neural networks and regression model", *Struct. Eng. Mech.*, **60**(4), 655-665.
- Alshihri, M.M., Azmy, A.M. and El-Bisy, M.S. (2009), "Neural networks for predicting compressive strength of structural light weight concrete", *Constr. Build. Mater.*, **23**, 2214-2219.
- Anagnostopoulos, A., Sideris, K.K. and Georgiadis, A. (2009), "Mechanical characteristics of self-compacting concretes with different filler materials exposed to elevated temperature", *Mater. Struct.*, **42**, 1393-1405.
- Annerel, E., Taerwe, L. and Vandeveld, P. (2007), "Assessment of temperature increase and residual strength of SCC after fire exposure", *The Fifth International RILEM Symposium on Self Compacted Concrete*, 715-720.
- Ashteyat, A.M., Haddad, R.H. and Ismeik, M. (2014), "Prediction of mechanical properties of post-heated self-compacting concrete using nondestructive tests", *Eur. J. Environ. Civil Eng.*, **18**, 1-10.
- Ashteyat, A.M., Ismeik, M. and Ramadan, K.Z. (2012), "Strength development models of concrete with silica fume as fine aggregate replacement material", *Glob. J. Res. Eng.*, **12**(2-A).
- Atici, U. (2011), "Prediction of the strength of mineral admixture concrete using multivariable regression analysis and an artificial neural network", *Exp. Syst. Appl.*, **38**, 9609-9618.
- Bakhtiyari, S., Allahverdi, A., Ghasemi, M.R., Zarrabi, B.A. and Parhizkar, T. (2011), "Self-compacting concrete containing different powders at elevated temperatures-mechanical properties and changes in the phase composition of the paste", *Thermochimica*, **514**, 74-81.
- Bilim, C., Atis, C.D., Tanyildizi, H. and Karahan, O. (2009), "Predicting the compressive strength of ground granulated blast furnace slag concrete using artificial neural network", *Adv. Eng. Softw.*, **40**, 334-340.
- Bouzoubaa, N. and Lachemi, M. (2001), "Self-compacting concrete incorporating high volumes of class F fly ash preliminary results", *Cement Concrete Res.*, **31**, 413-420.
- Camoses, A. and Martins, F.F. (2017), "Compressive strength prediction of CFRP confined concrete using data mining techniques", *Comput. Concrete*, **19**(3), 233-241.
- Chiang, C.H. and Yang, C.C. (2005), "Artificial neural network in prediction of concrete strength reduction due to high temperature", *ACI Mater. J.*, **102**, 93-102.
- Ding, Y., Azevedo, C., Aguiar, J.B. and Jalali, S. (2012), "Study on residual behavior and flexural toughness of fiber cocktail reinforced self compacting high performance concrete after exposure to high temperature", *Constr. Build. Mater.*, **26**, 21-31.
- Duan, Z.H. and Poon, C.S. (2014), "Factors affecting the properties of recycled concrete by using neural networks", *Comput. Concrete*, **14**(5), 547-561.
- Engin, S., Ozturk, O. and Okay, F. (2015), "Estimation of ultimate torque capacity of the SFRC beams using ANN", *Struct. Eng. Mech.*, **53**(5), 939-956.
- Fares, H., Noumowe, A. and Remond, S. (2009), "Self-consolidating concrete subjected to high temperature: Mechanical and physical properties", *Cement Concrete Res.*, **39**, 1230-1238.
- Fausett, L.V. (1994), *Fundamentals of Neural Networks: Architecture, Algorithms, and Applications*, Prentice Hall, New Jersey.
- Gregor, T., Franci, K. and Goran, T. (2009), "Prediction of concrete strength using ultrasonic pulse velocity and artificial neural networks", *Ultrasonic*, **49**, 53-60.
- Haddad, R.H., Odeh, R.A., Amawi, H.A. and Ababneh, A.N. (2013), "Thermal performance of self-compacting concrete: destructive and nondestructive evaluation", *Can. J. Civil Eng.*, **40**, 1205-1214.
- Haykin, S. (1999), *Neural Networks: A Comprehensive Foundation*, Prentice Hall, New Jersey.
- Ismeik, M. (2010), "Environmental enhancement through utilization of silica fume as a partial replacement of fine aggregate in concrete", *J. Civil Eng. Res. Pract.*, **7**(2), 11-21.
- Ismeik, M. and Al-Rawi, O. (2014), "Modeling soil specific surface area with artificial neural networks", *ASTM Geotech. Test. J.*, **37**, 678-688.
- Janotka, I. and Mojumdar, S.C. (2005), "Thermal analysis at the evaluation of concrete damage by high temperatures", *J. Therm. Anal. Calorim.*, **81**, 197-203.
- Kalifa, P., Chene, G. and Galle, C. (2001), "High-temperature behavior of HPC with polypropylene fibers from spalling to microstructure", *Cement Concrete Res.*, **31**, 1487-1499.
- Khalik, W. and Kodur, V. (2011), "Thermal and mechanical properties of fiber reinforced high performance self-consolidating concrete at elevated temperatures", *Cement Concrete Res.*, **41**, 1112-1122.
- Khayat, K.H., Bickley, J. and Lessard, M. (2000), "Performance of self consolidating concrete for casting basement and foundation walls", *ACI Mater. J.*, **97**, 374-380.
- Khurana, R. and Saccone, R. (2001), "Fly ash in self-compacting concrete", *ACI SP*, American Concrete Institute, Farmington Hills, Michigan, **99**, 259-274.
- Liu, X., Ye, G., De Schutter, G., Yuan, Y. and Taerwe, L. (2008), "On the mechanism of polypropylene fibers in preventing fire spalling in self-compacting and high performance cement paste", *Cement Concrete Res.*, **38**, 487-499.
- Neville, A.M. (1996), *Properties of Concrete*, Fourth Edition, Prentice Hall, New York.
- Noumowe, A., Carre, H., Daoud, A. and Toutanji, H. (2006), "High-strength self-compacting concrete exposed to fire test", *J. Mater. Civil Eng.*, **18**, 754-758.
- Persson, B. (2004), "Fire resistance of self-compacting concrete", *Mater. Struct.*, **37**, 575-584.
- Rumelhart, D.E., Hinton, G.E. and Williams, R.J. (1986), "Learning internal representation by error propagation. Parallel distributed processing: Explorations in the microstructure of cognition", Vol. 1, Eds. D.E. Rumelhart and J.L. McClelland, MIT Press, Cambridge.
- Siddique, R., Aggarwal, P. and Aggarwal, Y. (2011), "Prediction of compressive strength of self-compacting concrete containing bottom ash using artificial neural networks", *Adv. Eng. Softw.*, **42**, 780-786.
- Sonebi, M. (2004), "Application of statistical models in proportioning medium-strength self-consolidating concrete", *ACI Mater. J.*, **101**, 339-346.
- Sonebi, M., Grunewald, S., Cevik, A. and Walraven, J. (2016), "Modelling fresh properties of self-compacting concrete using Neural network technique", *Comput. Concrete*, **18**(4), 903-920.
- Tanyildizi, H. and Cevik, A. (2010), "Modeling mechanical performance of lightweight concrete containing silica fume exposed to high temperature using genetic programming", *Constr. Build. Mater.*, **24**, 2612-2618.
- Tao, J., Yuan, Y. and Taerwe, L. (2010), "Compressive strength of self-compacting concrete during high-temperature exposure", *J. Mater. Civil Eng.*, **22**, 1005-1011.
- Uysal, M. (2012), "Self-compacting concrete incorporating filler additives: Performance at high temperature", *Constr. Build.*

Mater., **26**, 701-706.

Uysal, M., Yilmaz, K. and Ipek, M. (2012), "Properties and behavior of self-compacting concrete produced with GBFS and FA additives subjected to high temperatures", *Constr. Build. Mater.*, **28**, 321-326.

Xu, Y., Wong, Y.L., Poon, C.S. and Anson, M. (2001), "Impact of high temperature on PFA concrete", *Cement Concrete Res.*, **31**, 1065-1073.

Yahia, A., Tanimura, M., Shimabkuro, A. and Shimoyama, Y. (1999), "Effect of rheological parameters on self compactability of concrete containing various mineral admixtures", *Proceeding of the First RILEM International Symposium on Self Compacting Concrete*, Stockholm, September.

AW

Nomenclature

	Symbol	Unit	Definition
<i>General</i>	ANN	-	artificial neural network
	SSC	-	self-compacted concrete
<i>Concrete ingredients</i>	C	kg/m ³	cement
	W	kg/m ³	water
	FA	kg/m ³	fine aggregate
	CA	kg/m ³	coarse aggregate
	WC	-	water-to-cement ratio
	SP	kg/m ³	super plasticizer dosage
<i>Filler types</i>	SF	kg/m ³	silica fume
	SG	kg/m ³	slag
	FAS	kg/m ³	fly ash
	M	kg/m ³	marble
	B	kg/m ³	basalt
	LS	kg/m ³	limestone
	G	kg/m ³	glass
	Q	kg/m ³	quartz
<i>Fiber types</i>	PP	kg/m ³	polypropylene
	ST	kg/m ³	steel fiber
<i>Environmental conditions</i>	RH	%	relative humidity
	T	C	temperature
<i>Output parameter</i>	RCS	%	residual compressive strength
<i>Variables</i>	X_i	-	input parameter
	\bar{X}	-	average value of input parameters
	Y_k	-	output parameter
	\bar{Y}	-	average value of output parameters
	Z_k	-	experimental result
	\bar{Z}	-	average value of experimental results
	R^2	-	coefficient of determination
<i>Statistical indices</i>	MAE	%	mean absolute error
	RMSE	%	root mean square error
	MAPE	%	mean absolute percentage error
	E	-	coefficient of efficiency